Rare Metal Materials and Engineering
Volume 49, Issue 8, August 2020
Available online at www.rmme.ac.cn

Science Press

Cite this article as: Rare Metal Materials and Engineering, 2020, 49(8): 2549-2556.

ARTICLE

Shock-induced Reaction Characteristics of Porous W/Zr-based Metallic Glass Composite Fragments

Zhang Yunfeng, Luo Xingbai, Liu Guoqing, Shi Dongmei, Zhang Yuling, Zhen Jianwei

Army Engineering University, Shijiazhuang 050000, China

Abstract: Quasi-sealed chamber tests were applied to W/Zr-based metallic glass composite, which is a novel form of multifunctional energetic structural material, to investigate its shock-induced reaction characteristics at various impact velocities. The influence of the cover plate thickness on the overpressure was also studied. Thermochemical theory of temperature controlled shock-induced chemical reactions was used to analyze the reaction characteristics of the material, as well as to identify the reaction parameters. The experimental and theoretical results show that the peak value of the quasi-static pressure is positively correlated with impact velocity of the fragments. The critical velocity to initiate the reaction is around 766 m/s. At a particular velocity, there is an optimal thickness of the cover plate to maximize the overpressure behind the plate. However, when the cover plate thickness is less than 8 mm, the overpressure behind the plate is relatively small. The critical shock pressure P_c to initiate the chemical reaction is about 18.37 GPa. The theoretical critical shock temperature T_c is calculated to be 3736.6 K. The theoretical results show that the reaction efficiency in the chamber increases as the shock pressure or temperature increases. The theoretical reaction efficiency reaches 61.5% when the shock pressure is 40 GPa, indicating that the chemical reactions of the material do not run to completion in the experiments.

Key words: multifunctional energetic structural material; porous W/Zr-based metallic glass composites; shock-induced chemical reaction; energy release characters

Multifunctional energetic structural materials (MESMs) are a special class of materials with structural and energetic characteristics that can improve the damage effectiveness of warhead systems [1]. A shock-induced chemical reaction (SICR) will occur when the material achieves certain states, such as high pressure, high temperature or high speed impact. And an unsupported reaction will decay to zero unless certain conditions are met [2,3]. Due to their mechanical strength and energetic characteristics, MESMs are widely used in military applications such as shaped charge liners[4], energetic fragments[5,6] and reactive kinetic energy penetrators[7]. These materials may include thermite mixtures, intermetallic compounds, metal-polymer mixtures, metastable intermolecular composites, as well as hydrides[8,9]. Porous W/Zr-based metallic glass composite, whose strength is much higher than that of other traditional MESMs, possesses desired energy release characteristics and is a valuable new kind of MESMs. However, relatively little research has been reported on the shock-induced reaction characteristics of the material.

When MESMs fragments impact a target, the propagated shock waves generate a temperature rise within the fragments, which takes up the shock energy in the fragments. The heated fragments will then react when the shock energy is larger than the critical energy[10]. The energy released by chemical reactions in the material greatly increases the damage that the fragments can cause. Therefore, it is important to investigate the shock-induced chemical-reaction (SICR) characteristics of the material. The shock pressure responses of Ni/Al and Ni/Ti powder mixtures[11-13], as well as SICRs and syntheses of Ni/Al powder mixtures[14,15], have been systematically studied

Received date: August 22, 2019
Corresponding author: Liu Guoqing, Ph. D., Professor, Shijiazhuang Campus, Army Engineering University, Shijiazhuang 050000, P. R. China, E-mail: 1193954881@qq.com

by Thadhani et al. However, their work lacks quantitative results of the SICRs of the materials. Recently, a quasi-sealed chamber developed by Ames[16] has been extensively applied in studying SICRs, making it possible to evaluate the reaction efficiency of the MESMs by measuring the shock over-pressure in the chamber. For most energetic materials, the reaction initiation mechanisms are controlled by the rise of shock temperature. Clearly, the shock temperature is controlled by the input stress, which is in turn directly influenced by impact velocity, and the reaction efficiency itself is strongly dependent on impact velocity, which governs shock pressure, for most MESMs[8]. The SICR's energy-release characteristics as well as the venting effects of accumulated roll-bonding of Ni/Al polymer-bonded explosive materials were investigated by Ji et al[17], Cai et al[18], and Wang et al[19]. Xiong et al[20] presented the effects of two additives, namely Teflon and copper, on the mechanical properties and SICR characteristics of Al/Ni material. Wang et al[21] presented a novel modified quasi-sealed chamber and discussed the SICR behavior of Zr-based bulk metallic glass. It is worth noting that the thickness of the plate also has an influence on the energy release of the MESM, as reported by Xu et al[22].

To further analyze the SICR characteristics of the materials and to explain their reaction mechanism, significant theoretical work has been done by many researchers. Boslough[2] developed a description of SICR based on fundamental thermochemical and shock wave principles. By comparing the measured and calculated temperatures of porous thermite, the existence of SICRs was verified. A thermochemical model of temperature controlled shock-induced chemical reactions in MESMs was established by Zhang et al[9]. The shock equation of state, including chemical reactions, Arrhenius equation, and the Avrami-Erofeev model were taken into consideration in this model. From the proposed theory, the temperature rises along with shock temperature and thermochemical reaction can be accurately calculated. The shock temperatures and reaction efficiencies of a Ni/Al system with two additives were obtained from this theory, and the reaction constants have been calculated[23].

In order to investigate the energy release characteristics of porous W/Zr-based metallic glass composite due to a shock-induced chemical reaction, we have measured the overpressures generated by impacting the fragments at various velocities, as well as the overpressures behind the plate with different thicknesses of cover plates using the quasi-sealed chamber tests. Further, we theoretically discussed the effects of initial conditions on the reaction efficiencies using the Arrhenius equation and the Avrami-Erofeev model, and compared the calculated values with experimental data. The results indicate that shock pressures or temperatures have a positive influence on the reaction efficiencies within a certain range of impact velocities.

1 Experiment

1.1 Experimental materials

$Zr_{53.5}Cu_{26.5}Ni_5Al_{12}Ag_3$ bulk metallic glass (BMG) was used as the composite matrix. The BMG ingots were prepared by melting and combining raw materials (purity 99.8%) in a Ti-gettered high-purity argon atmosphere. Each ingot must be flipped at least four times to ensure good homogeneity of ingredients. The porous W with 3D net structure, with actual porosity of 38.4%, was fabricated by powder sintering, and the porosity was assured by the volume fraction of agglutinant. The alloy ingot was inserted into the mold containing porous tungsten by employing the vacuum infiltration technology. After pressing for a few minutes, the mold was cooled with saturated salt water so that amorphous phases could be readily formed. The actual density of the material was 14.5 g/cm^3. Cylindrical fragments with 8 mm in diameter and 9 mm in height were made by machining.

Fig.1 shows a micrograph of the morphology of the material delineated by SEM. The porous tungsten has a 3D net structure and a relatively high volume fraction. The grey phase therefore represents porous tungsten. The dark metallic glass phase is dispersed and squeezed uniformly in the porous tungsten. No crystal phase is separated out in the metallic glass phase and the interface bonding is favorable. The formation and propagation of the shear bands of metallic glass can be prevented by the porous tungsten, which leads to high plasticity and fracture strength of the composite [24,25].

1.2 Experimental layout

The impact-initiation experimental layout configuration used in this investigation is shown in Fig.2. Porous W/Zr-based metallic glass composite fragments along with nylon sabots were shot by a 14.5 mm ballistic gun that was 5 m away from the cover plate in front of the quasi-sealed chamber. The nylon sabots had grooves to ensure that they could break and separate during flight. The range of velocities in the tests was from 700 m/s to 1400 m/s, controlled by adjusting the mass of the propellant. The velocity measurement system consisted of two aluminum foils; a time recorder was used to infer the velocities of the fragments. The enclosed volume of the chamber was 35.2 L. The mild steel cover plates with four

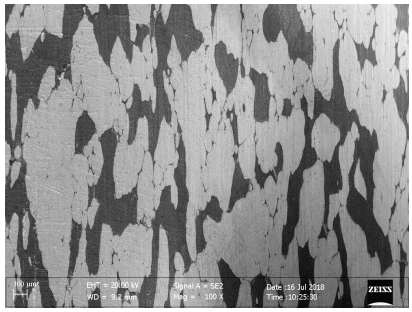

Fig.1 SEM image of porous W/Zr-based metallic glass composite

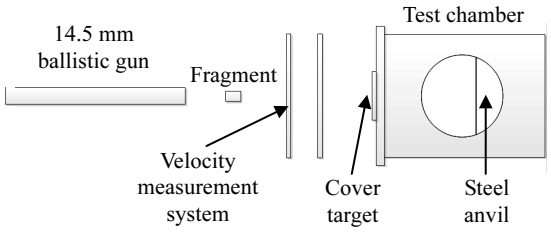

Fig.2 Schematic illustration of the setup for quasi-sealed chamber test

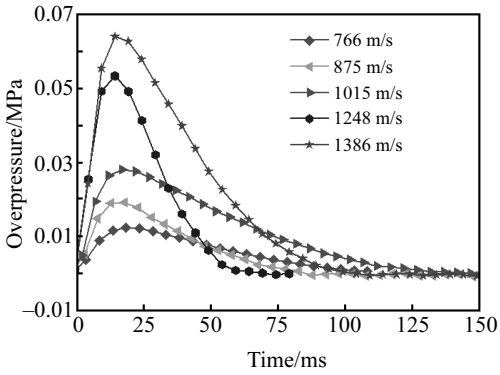

Fig.3 Pressure as a function of time for a 0.5 mm cover plate at different impact velocities

thicknesses, namely 0.5, 2, 4, and 8 mm, were fixed in the front of the chamber and a 30 mm thick hardened steel anvil was welded to the bottom of the chamber. The overpressures generated by fragments penetrating the cover plates and impacting the anvil were recorded by a transient pressure sensor fixed inside the chamber. The threshold of the sensor was set to be 3.9 mV, corresponding to an overpressure of 0.001 56 MPa in the chamber. The SICR behavior of the fragments was observed by aiming a high-speed camera at the mirror in the chamber. The framing rate was 10 000 frames/s (100 μs per frame).

2 Results and Discussion

2.1 Overpressures in the chamber

The data of a series of impact initiated experiments are listed in Table 1, including impact velocity v, fragment mass m, thickness of cover plates h, and peak value of the quasi-static pressure ΔP. The slash mark "/" means that it is not detected, and the ΔP of this shot is less than the threshold of the sensor. Usually, the impact velocity corresponding to the minimum ΔP that can be detected is regarded as the critical velocity v_c of the SICR. From these experimental data, it can be inferred that the critical velocity of the SICR of porous W/Zr based metallic glass composite fragments is around 766 m/s.

Fig.3 illustrates time history of the quasi-static pressure in the chamber with a 0.5 mm cover plate at different velocities. Because the time scale for the fragments to impact the anvil and reactions to occur is relatively short, tone sees dramatic increase in pressure at the beginning of the curves, i.e., the ignition stage. The inflated air ejecting from the holes which are generated by the penetration of fragments on the cover plates results in the gradual drops of the curves during the venting stage. The pressure-rising stage takes several milliseconds; the pressure-dropping to the ambient pressure takes up to hundreds of milliseconds[19]. It is evident that the peak pressures ΔP have obvious correlations with impact velocities. Both ΔP and its rate of increase grow larger as the impact velocity increases. This tendency is the same as the behavior of the ZrCuNiAl BMG fragments obtained by Wang et al[21].

Table 1 Experimental data of SICR

Shots	v/m·s^{-1}	m/g	h/mm	ΔP/MPa
17#	753	6.75	0.5	/
18#	766	6.62	0.5	0.012
19#	875	6.60	0.5	0.019
20#	1015	6.59	0.5	0.028
22#	1248	6.72	0.5	0.053
23#	1386	6.37	0.5	0.063
30#	1238	6.33	2	0.051
31#	1257	6.37	4	0.055
32#	1242	6.38	8	0.047

Fig.4 shows time history of the quasi-static pressure in the chamber with different cover plates at velocities around 1250 m/s. For this impact velocity, the maximum peak overpressure is generated when impacting the 4 mm steel cover plate. There is presumably an optimum plate thickness to maximize the behind-plate overpressure effect for the porous W/Zr based metallic glass composite fragments, similar to the overpressure effect for PTFE/Al/W reactive material[22]. Nonetheless, compared with other MESMs, the influence of plate thickness on the overpressure for the material is relatively small. The venting time of the inflated air in the chamber is related to the thickness of the cover plate. It takes tens of milliseconds for the overpressure to drop to zero with the 0.5 mm cover plate, but hundreds of milliseconds with a 2 mm cover plate. Fig.5 shows the shapes of the holes created by fragments penetrating 0.5 and 2 mm cover plate. The deformation and size of the hole are larger for the 0.5 mm cover plate, leading to a more rapid leaking of gas. For the 2 mm cover plate, the deformation and size of the hole are relatively small, resulting in long venting time.

2.2 Shock-induced chemical reaction behavior

The high speed camera video frames of the SICR process for the shot 17# fragment are shown in Fig.6. The time of the first frame when the fragment impacts the cover plate is defined as t=0 ms. A small part of the fragment begins to fracture and react when impacting and perforating the cover plate, as illustrated in Fig.6a. As shown in Fig.6b and 6c, no

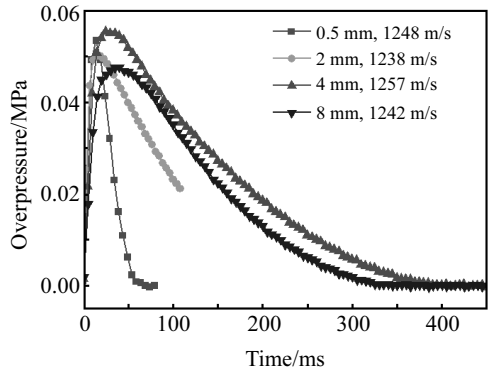

Fig.4 Overpressure as a function of time for different cover target thicknesses

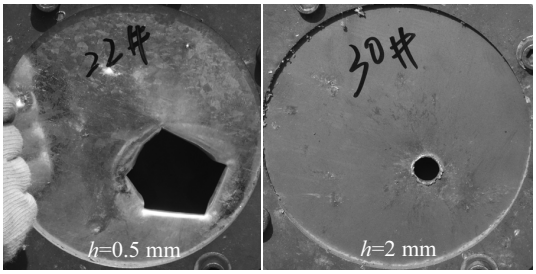

Fig.5 Penetrated cover targets

flame can be observed before the residual fragment impacts the steel anvil, which indicates that the impact of the fragment on the cover plate drives no sequential chemical reactions. Once impacting the steel anvil, the reaction is initiated but the range of the flame is relatively small, as shown in Fig.6d. This shot does not trigger the transient pressure sensor, which means that the produced overpressure is less than the threshold and the reaction is unsustainable. The SICR behavior of MESMs is complex processes combining impact kinetics and thermochemical responses. The unsupported reactions will decay to zero unless certain conditions are met, such as high pressure, high temperature, or high speed-impact. The velocity of shot 17# is obviously less than the critical velocity.

Fig.7 shows the high-speed camera video frames of the SICR process for the shot 22# fragment. The SICR process in the quasi-sealed chamber test involves three main steps. (1) A small part of the fragment begins to fracture and react when impacting and perforating the cover plate, as illustrated in Fig.7a. (2) After the fragment passes through the cover plate, it continues to reach the steel anvil, deflagration occurs, and the flame is visible, as illustrated in Fig.7b. (3) The strong reaction induced by the fragment impacting on the anvil produces a roughly hemispherical deflagration wave on the interior. This wave then begins to propagate and reflect in the chamber, resulting in an increase in the overpressure, as shown in Fig.7c and 7d.

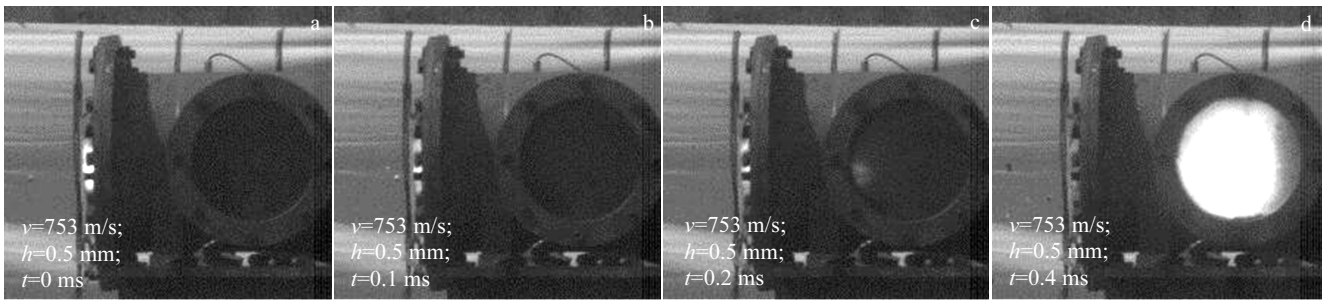

Fig.6 High-speed images of SCIR process for the shot 17# fragment: (a) t=0 ms, (b) t=0.1 ms, (c) t=0.2 ms, and (d) t=0.4 ms

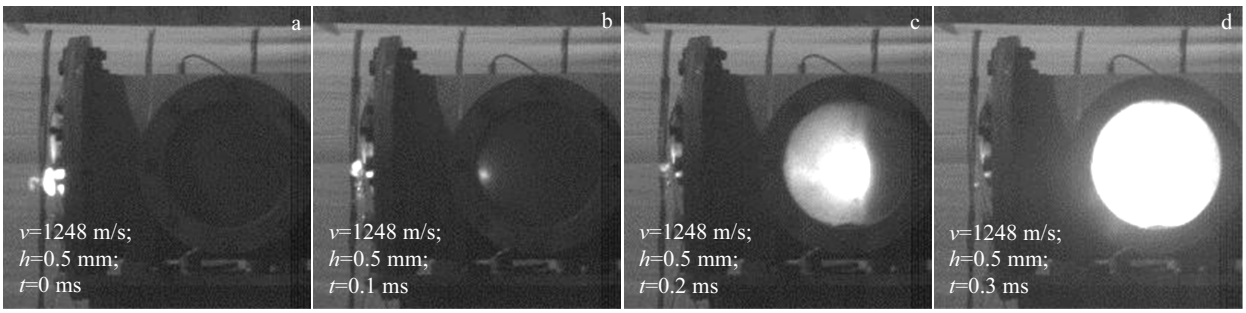

Fig.7 High-speed images of SCIR process for the shot 22# fragment: (a) t=0 ms, (b) t=0.1 ms, (c) t=0.2 ms, and (d) t=0.3 ms

The sequence of events for the shot 32# fragment is similar to that for the shot 22# fragment, as shown in Fig.8. The fragment is fractured into a few parts, which penetrate the thick cover plate. The debris of the fragment begins to react and splash outside the chamber, as demonstrated in Fig.8a and 8b. The activated fragment continues, impacting the steel anvil and triggering a more intense reaction. The hemispherical deflagration wave propagates from the bottom to the front of the chamber, as shown in Fig.8c and 8d. The degree of fragmentation and the total chemical energy released inside the chamber are influenced by the thickness of the cover plate. However, because of the high strength of the material, the influence of plate thickness on the overpressure for the material is relatively small compared with that of other MESMs[24,26].

3 Discussions

3.1 Reaction efficiencies

The initial shock pressures of the fragment and the plate are equal at the moment of impact. According to the conservation laws of momentum and energy, the shock pressure of fragment and target is given by follows [26,27]:

$$p_{\mathrm{H}} = \rho D u \tag{1}$$

where p_{H} is the shock pressure, ρ, D and u are the density, shock wave velocity, and particle velocity of the material or steel target, respectively. The particle velocity of the target can be found from basic shock wave theory[28]:

$$u_2 = \frac{-\left(\rho_2 C_2 + \rho_1 C_1 + 2\rho_1 s_1 v\right) \pm \Delta^{1/2}}{2\left(\rho_2 s_2 - \rho_1 s_1\right)} \tag{2}$$

where C, s are the Hugoniot parameters, and subscripts 1 and 2 refer to the MESM and the target, respectively; Δ can be written as[29]:

$$\Delta = \left(\rho_2 C_2 + \rho_1 C_1 + 2\rho_1 s_1 v\right)^2 + 4\rho_1\left(\rho_2 s_2 - \rho_1 s_1\right)\left(C_1 v + s_1 v^2\right) \tag{3}$$

Because it takes only several milliseconds after the onset of the primary reaction for the quasi-static pressure to reach its peak value, the mass and energy flux from the chamber can be neglected. The relationship between the peak value of the overpressure in the chamber and the energy deposition can be described as follows[23]:

$$\Delta P = \frac{\gamma - 1}{V}\Delta Q \tag{4}$$

where V is the volume of the chamber, ΔQ is the energy deposition, and γ=1.4 is the ratio of the specific heats of the gas in the chamber.

The energy deposited in the chamber consists of the kinetic energy of the fragments and the chemical energy resulting from the chemical reaction in the material. The kinetic energy of the fragment is 1913.66 J as the velocity is 753 m/s, and the sensors have not yet detected the overpressure in the chamber at this time. Therefore, the kinetic energy of the fragments has very little influence on the energy deposition in the chamber, which indicates that the kinetic energy can be neglected in the calculations.

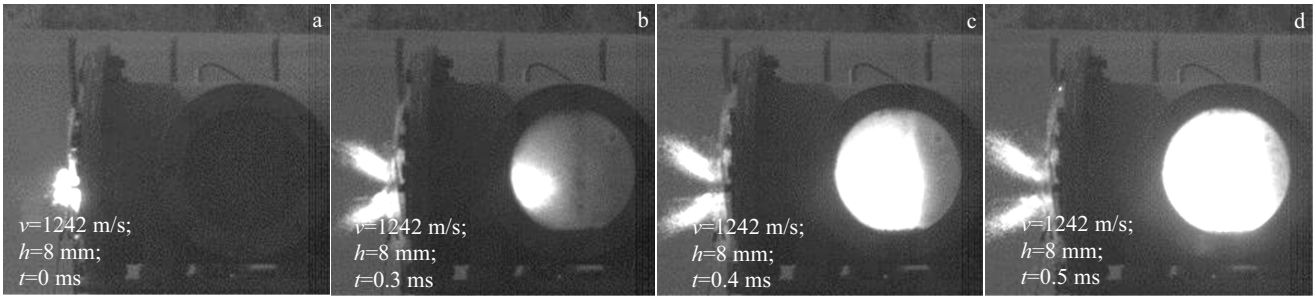

Fig.8 High-speed images of SCIR process for the shot 32# fragment: (a) t=0 ms, (b) t=0.3 ms, (c) t=0.4 ms, and (d) t=0.5 ms

The reaction enthalpies of the SICR for the material are as follows[21].

$Zr+O_2 \rightarrow ZrO_2$, ΔH=11849.1 J/g

$Al+Ni \rightarrow NiAl$, ΔH=1381.33 J/g

$Al+O_2 \rightarrow Al_2O_3$, ΔH=31 053 J/g

According to the work of Eakins et al[12], NiAl is the most common reaction product when Ni and Al react in the SICRs. The rest of the aluminum reacts with oxygen, and the effects of Cu, Ag, and W can be neglected. Therefore, the theoretical energy is calculated to be 1469.4 J/g. Table 2 demonstrates the theoretical shock pressures, energy depositions, and reaction

Table 2 Calculated results based on experimental data

Shots	v/ m·s^{-1}	h/ mm	P/ GPa	ΔQ/ kJ	Theoretical chemical energy/kJ	Reaction efficiency/%
18#	766	0.5	18.37	1.02	9.73	10.48
19#	875	0.5	21.38	1.67	9.70	17.22
20#	1015	0.5	25.38	2.42	9.68	25.00
22#	1248	0.5	32.41	4.63	9.87	46.91
23#	1386	0.5	36.79	5.54	9.36	59.19
30#	1238	2	32.10	4.49	9.30	48.28
31#	1257	4	32.70	4.84	9.36	51.71
32#	1242	8	32.23	4.14	9.37	44.18

efficiencies based on the experimental data. These numbers reveal that the reaction efficiency increases as the impact velocity and shock pressure increase. When the impact velocity of the fragment is 1386 m/s, the shock pressure and reaction efficiency reach 38.78 GPa and 59.19%, respectively. The values of C_1, s_1, C_2, s_2, and ρ_2 are 3.417 km/s, 1.732, 4.57 km/s, 1.49, and 7.85 g/cm^3 in the computation, respectively.

3.2 Theoretical calculations for SICR

From the Grunesien equation of state (EOS) and Rankine-Hugoniot energy equation, the *p*-*V* form of the EOS for solids can be written as [29]:

$$p(V)=\frac{\frac{V}{\gamma(V)}p_c(V)-E_c(V)}{\frac{V}{\gamma(V)}-\frac{1}{2}(V_0-V)} \tag{5}$$

where V is the specific volume, V_0 is the initial specific volume of solid, γ represents the Grunesien coefficient, and P_c and E_c are the cold pressure and cold internal energy, respectively. According to the Mayer potential energy, the *Q*-*q* form of the internal energy and cold pressure can be described as follows[27]:

$$E_c(\delta)=\frac{3Q}{\rho_{0\,K}}\left\{\frac{1}{q}\exp\left[q\left(1-\delta^{-1/3}\right)\right]-\delta^{-1/3}-\frac{1}{q}+1\right\} \tag{6}$$

$$p_c(\delta)=Q\delta^{2/3}\left\{\exp\left[q\left(1-\delta^{-1/3}\right)\right]-\delta^{2/3}\right\} \tag{7}$$

where Q and q are two parameters for cold energy, $\delta=\rho/\rho_{0\,K}=V_{0\,K}/V$ is the compressibility at 0 K for the material, and $\rho_{0\,K}$ and $V_{0\,K}$ are the density and specific volume at 0 K, respectively. The Dugdale-MacDonald relationship for the Grunesien coefficient can be written as follows[27]:

$$\gamma(V)=\frac{1}{6}\frac{q^2\delta^{-1/3}\exp\left[q\left(1-\delta^{-1/3}\right)\right]-6\delta}{q\exp\left[q\left(1-\delta^{-1/3}\right)\right]-2\delta} \tag{8}$$

The material parameters Q and q can be found using the theoretical method developed by Hu et al[30]:

$$s_{0\,K}=\frac{1}{12}\frac{q^2+6q-18}{q-2} \tag{9}$$

$$C_{0\,K}^2=\frac{Q(q-2)}{3\rho_{0\,K}} \tag{10}$$

$$C_{0\,K}=C_0\left[1+\left(2s-\frac{\gamma_{0\,K}^2}{4}-1\right)\alpha_V T_0\right] \tag{11}$$

$$s_{0\,K}=s_0\left[1+\left(\frac{s}{2}-\frac{1}{8}\frac{\gamma_{0\,K}^2}{s}-1\right)\alpha_V T_0\right] \tag{12}$$

where $C_{0\,K}$, $s_{0\,K}$, and $\gamma_{0\,K}$ are the Hugoniot parameters and Grunesien coefficient at 0 K, C_0 is the zero-pressure bulk sound speed at the initial temperature, $\alpha_V=1.559\times10^{-5}$ K^{-1} is the coefficient of cubic expansion, and $T_0=298$ K is the initial temperature.

According to the relationship between the isentrope and Hugoniot, assuming that the specific heat at constant volume and γ/V are both constant, the equation for shock temperature is reduced to the relatively simple form[2]:

$$T_H=T_0\exp\left(-\int_{V_0}^{V_H}\frac{V}{\gamma}\mathrm{d}V\right)+\frac{V}{\gamma}\frac{p_H-p_S}{C_V} \tag{13}$$

where T_H is the shock temperature, $C_V=0.2074$ J·g^{-1}·K^{-1} is the specific heat at constant volume of the material, and p_s is the isentrope, which can be described as follows[27]:

$$p_s(\eta)=\rho_0C_0^2\exp(\gamma_0\eta)\int_0^\eta\frac{\left(1+(s-\gamma_0)\right)x}{(1-sx)^3}\exp(-\gamma_0x)\mathrm{d}x \tag{14}$$

where $\eta=1-V/V_0$ is the compressibility, ρ_0 is the initial density of the material, and $\gamma_0=1.553$ is the initial Grunesien coefficient. Combining Eq.(7) and Eq.(15), the relationship between shock pressure and shock temperature can be deduced.

Assuming that the chemical process depends on temperature only, the thermal kinetics formula for the solid-state reaction can be improved using the Arrhenius model[9]:

$$\frac{\mathrm{d}y}{\mathrm{d}t}=A\exp\left(-\frac{E_a}{R_uT}\right)f(y) \tag{15}$$

where y is the reaction efficiency, t is the reaction time, A is the apparent pre-exponential factor, E_a is the apparent activation energy, and R_u and T are the universal gas constant and the absolute temperature, respectively. An *n*-dimensional Avrami-Erofeev equation is suitable to model the solid-state reaction based on the works of Zhang et al [9].

$$f(y)=n(1-y)\left[-\ln(1-y)\right]^{(n-1)/n} \tag{16}$$

where n is the coefficient related to boundary conditions and reaction mechanisms. The Avrami-Erofeev equation can be written as the first derivative of absolute temperature T with respect to the efficiency of reaction y as follows [9]:

$$\frac{\mathrm{d}T}{\mathrm{d}y}=\frac{R_uT^2}{E_a}\left[\frac{1}{2y}-\frac{n\ln(1-y)+n-1}{n(1-y)\left[-\ln(1-y)\right]}\right] \tag{17}$$

In order to find the theoretical reaction efficiency of the material, the corresponding pressure, temperature, and reaction efficiency achieved in the experiment can serve as the threshold of the SICR, namely the critical pressure $P_c=18.37$ GPa, the critical temperature $T_c=3736.6$ K, and relevant reaction efficiency $y_c=10.48\%$. The quantities E_a and n are fitted from the SICR experimental results for the porous W/Zr based metallic glass composite. The values of E_a and n are 517.06 kJ and 0.2611, respectively. Fig.9 and Fig.10 show the reaction efficiency as a function of shock pressure and shock temperature, respectively. These graphs show that the theoretical results are close to the experimental data, indicating that the theoretical method and reaction parameters can effectively describe the principle SICR characteristics for the material. The relation between the reaction efficiency and the

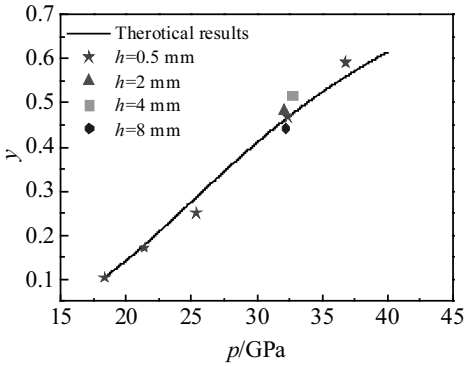

Fig.9 Reaction efficiency as a function of shock pressure

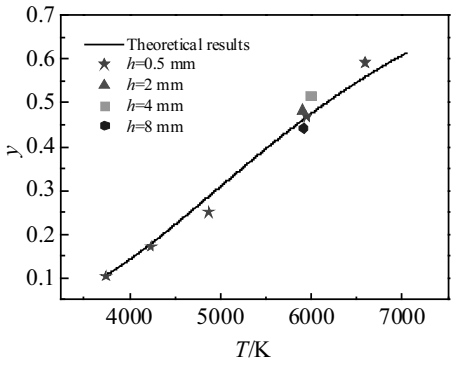

Fig.10 Reaction efficiency as a function of shock temperature

shock pressure or shock temperature is almost linear when the shock pressure is less than 40 GPa. The thickness of the cover plate has relatively little effect on the detected released energy if its thickness is less than 8 mm. Even when the impact pressure attains 40 GPa, the chemical reaction is not completed, and the corresponding reaction efficiency reaches 61.5%. These numbers demonstrate that the porous W/Zr based metallic glass composite is relatively insensitive.

4 Conclusions

1) The impact-initiated experiments and thermal kinetics analysis are performed to investigate its shock-induced chemical reaction (SICR) characteristics under different impact velocities and different cover plate thicknesses.

2) A violent chemical reaction is initiated once the material undergoes high-speed impact. The critical velocity of the SICR for the material is around 766 m/s, and the corresponding theoretical critical pressure P_c and critical temperature T_c are 18.37 GPa and 3736.6 K, respectively.

3) The relationship between the reaction efficiency and shock pressure or shock temperature are discussed according to the Arrhenius model and the Avrami-Erofeev equation. The results show that the theoretical method is valid for describing the SICR characteristics of the material. The value of the apparent activation energy E_a=517.06 kJ and coefficient n=0.2611 for the SICR of the material are calculated. There is a positive correlation between the reaction efficiency and the shock pressure or shock temperature when the shock pressure is less than 40 GPa.

4) The thickness of the cover plate has relatively little effect. The porous W/Zr based metallic glass composite is relatively insensitive, and the reactions in the experiments do not run to completion.

References

1 Zhang Xianfeng, Zhao Xiaoning. *Chinese Journal of Energetic Materials*[J], 2009, 17(6): 731 (in Chinese)

2 Boslough M B. *The Journal of Chemical Physics*[J], 1990, 92(3): 1839

3 Bennett L S, Horie Y. *Shock Waves*[J], 1994, 4: 127

4 Walter W P, Kecskes L J, Pritechett J E. *23rd International Symposium on Ballistics Tarragona*[C]. New Jersey: IEEE, 2007: 31

5 Xu F Y, Zheng Y F, Yu Q B *et al*. *International Journal of Impact Engineering*[J], 2016, 95: 125

6 Xu F Y, Yu Q B, Zheng Y F *et al*. *International Journal of Impact Engineering*[J], 2017, 104: 13

7 Conner R D, Dandliker R B, Scruggs V *et al*. *International Journal of Impact Engineering*[J], 2000, 24: 435

8 Zhang X F, Shi A S, Qiao L *et al*. *Journal of Applied Physics*[J], 2013, 113: 83 508

9 Zhang X F, Shi A S, Zhang J *et al*. *Journal of Applied Physics*[J], 2012, 111: 123 501

10 Luo P G, Wang Z C, Jiang C L *et al*. *Materials and Design*[J], 2015, 84: 72

11 Eakins D E, Thadhani N N. *Journal of Applied Physics*[J], 2007, 101: 43 508

12 Eakins D E, Thadhani N N. *Acta Materialia*[J], 2008, 56: 1496

13 Specht P E, Thadhani N N, Weihs T P. *Journal of Applied Physics*[J], 2012, 111: 73 527

14 Xu X, Thadhani N N. *Journal of Applied Physics*[J], 2004, 96(4): 2000

15 Eakins D E, Thadhani N N. *Journal of Applied Physics*[J], 2006, 100: 113 521

16 Ames R G. *43rd AIAA Aerospace Science Meeting and Exhibit*[C]. New Jersey: IEEE, 2005: 279

17 Ji C, He Y, Wang C T *et al*. *Materials and Design*[J], 2017, 116: 591

18 Cai X M, Zhang W, Xie W B *et al*. *Materials and Design*[J], 2015, 68: 18

19 Wang H F, Zheng Y F, Yu Q B *et al*. *Journal of Applied Physics*[J], 2011, 110: 74 904

20 Xiong W, Zhang X F, Wu Y *et al*. *Journal of Alloys and Compounds*[J], 2015, 648: 540

21 Wang C T, He Y, Ji C *et al*. *Intermetallics*[J], 2018, 93: 383

22 Xu F Y, Geng B Q, Zhang X P *et al*. *Propellants, Explosives, Pyrotechnics*[J], 2017, 42: 192

23 Xiong W, Zhang X F, Tan M T *et al*. *The Journal of Physical Chemistry*[J], 2016, 120: 24 551
24 Xue Y F, Cai H N, Wang L *et al*. *Materials Science and Engineering A*[J], 2007, 445: 275
25 Zhang X Q, Wang L, Xue Y F *et al*. *Materials Science and Engineering A*[J], 2013, 561: 152
26 Jing F Q. *Experimental State Equation Guidance*[M]. Beijing: Science Press, 1999: 209
27 Tan H. *Introduction to Experimental Shock-wave Physics*[M]. Beijing: National Defence Industry Press, 2007: 15
28 Zhang Xianfeng, Zhao Xiaoning, Qiao Liang. *Explosion and Shock Waves*[J], 2010, 30(2): 145 (in Chinese)
29 Zhang X F, Qiao L, Shi A S. *Journal of Applied Physics*[J], 2011, 110(1): 13 506
30 Hu Jinbiao, Jin Fuqian. *Chinese Journal of High Pressure Physics*[J], 1990, 4(3): 175 (in Chinese)

W 骨架/Zr 基非晶合金复合材料破片的冲击释能特性

张云峰，罗兴柏，刘国庆，施冬梅，张玉令，甄建伟
(陆军工程大学，河北 石家庄 050000)

摘　要：W 骨架/Zr 基非晶合金复合材料是一种新型含能结构材料。采用准密封箱冲击超压实验，研究了 W 骨架/Zr 基非晶合金复合材料的在不同冲击速度下和靶板厚度下的冲击释能特性。并根据温度控制含能结构材料冲击诱发化学反应的热动力学理论，确定了材料的化学反应参数，分析了材料的热化学反应特性。结果表明，材料冲击超压峰值与冲击速度正相关，其激发反应阈值为 766 m/s，在相同速度下，有使破片靶后释能效率最大化的最优靶板厚度，但在 8 mm 厚钢靶范围内，前板厚度对冲击释能特性影响不大。材料冲击激发化学反应的冲击压力阈值 P_c=18.37 GPa，对应的理论温度阈值 T_c=3736.6 K。材料反应效率随着冲击压力和击波温度的增加而增加，在 40 GPa 冲击压力范围内，材料并未完全反应，其理论反应效率达到 61.5%。

关键词：含能结构材料；W 骨架/Zr 基非晶合金复合材料；冲击诱发化学反应；释能特性

作者简介：张云峰，男，1990 年生，博士生，陆军工程大学石家庄校区，河北 石家庄 050000，E-mail: 1193954881@qq.com